On the Accuracy of Automotive Radar Tracking

Lennert Jacobs, Peter Veelaert, Heidi Steendam and Wilfried Philips
TELIN-IPI, Ghent University - imec
St-Pietersnieuwstraat 41, B-9000 Gent, Belgium
Email: {lennert.jacobs, peter.veelaert, heidi.steendam, wilfried.philips}@ugent.be

2023 IEEE 97th Vehicular Technology Conference (VTC2023-Spring) | 979-8-3503-1114-3/23/$31.00 ©2023 IEEE | DOI: 10.1109/VTC2023-Spring57618.2023.10200523

***Abstract*—Radar has become a key sensor in many advanced driver assistance systems (ADAS). Due to its excellent range and Doppler resolution, low cost, and robustness against environmental conditions, it is considered an attractive sensor for detecting and tracking vulnerable road users (VRUs). In this paper, we provide a theoretical analysis of the accuracy of radar based VRU detection and tracking systems, thereby focusing on a number of specific scenarios such as early detection and tracking of VRUs, a VRU crossing the road at constant speed in front of a vehicle, a VRU moving parallel to a vehicle, etc. More specifically, we derive the Cramer-Rao lower bound (CRLB) for position and velocity estimation of a moving target based on a sequence of noisy range, azimuth, and Doppler measurements taken from a moving ego-vehicle equipped with one or multiple radars. Not only does the CRLB serve as a benchmark to evaluate the performance of any practical tracking algorithm, it also allows to gain practical insights regarding the impact of the radar setup and configuration on the tracking accuracy in different realistic scenarios. Furthermore, we show that the generalized least-squares estimator (GLSE) achieves excellent performance when few measurements are available, and propose a novel active sensing (AS) application based on the CRLB where the radar configuration is optimized on the fly to improve either tracking accuracy or computational efficiency.**

***Index Terms*—automotive radar, tracking accuracy**

I. Introduction

Because of its low cost and robustness against environmental conditions like rain, snow, fog, dust, dirt, darkness, or glaring sun, mmWave radar has become a key sensor in many advanced driver assistance systems (ADAS), such as emergency brake, blind spot detection, and detection and tracking of vulnerable road users (VRUs) [1], [2]. State-of-the-art automotive radar sensors are known to provide excellent range and Doppler resolution, but poor angular resolution due to the limited number of antennas in the (virtual) antenna array. In order to accurately track moving VRUs from imperfect (radar) detections, recursive Bayesian filters such as Kalman filters (KFs) or Particle filters (PFs) have been well established. By assuming that the state of a tracked object evolves according to a Markov process, recursive Bayesian filters allow a computationally and memory efficient two-step implementation: in the prediction step, the current state is predicted from the previous state and a prescribed dynamic model, whereas in the update step, the state prediction is updated using the current measurement (if available) and an observation model. In order to model a maneuvering target's deviation from the dynamic model, additive process noise is injected at the prediction step. Since a single dynamic model is often not sufficient to describe the target's movement at all times, an interacting multiple model (IMM) approach can be used where multiple recursive Bayesian filters operate in parallel, each with their own dynamic model [3]. Any estimator for a nonlinear filtering problem under the Bayesian framework is lower bounded by the Bayesian or posterior Cramer-Rao lower bound (PCRLB) [4]–[6]. However, since the PCRLB involves taking the expectation over the joint probability density of both the observations and the random state parameters, the useful measurement information has been averaged out and the PCRLB becomes an offline bound [7] that does not properly address the tracking performance for a particular trajectory. In [8], the performance of the current realization of the tracker is shown to be more accurately bounded by the predicted conditional Cramer-Rao lower bound (PC-CRLB), which is conditioned on past measurements. In numerous recent papers [9]–[11], the PC-CRLB has been adopted to implement dynamic and real-time resource management in large-scale (MIMO) radar networks.

In the context of VRU safety systems, however, it is essential to be able to assess the tracking performance in a number of important and well-defined scenarios of interest, e.g., a pedestrian crossing at constant speed in front of a vehicle, a VRU moving parallel to a vehicle turning left, early detection and tracking of VRUs based on a small number of measurements. As many of these scenarios can be sufficiently well described by a deterministic dynamic model, the unknown parameters are now deterministic and classical estimators can be used instead of Bayesian filters. The variance of any unbiased estimator is known to be lower bounded by the conventional Cramer-Rao lower bound (CRLB). In the literature, the CRLB is typically used for target localization accuracy from a single radar measurement [12]–[14]. The CRLB for position estimation from successive radar measurements has been derived mainly in the context of air traffic control (ATC). In [15], the CRLB for position and velocity estimation of a single target in a horizontal plane using range and azimuth measurements was derived under the assumption of temporally white Gaussian noise. The positive impact of adding Doppler measurements to the tracker in 3D space was shown in [16]. Ignoring the impact of ego-motion, the theoretical CRLB was computed in [17] for various single and multi-sensor system setups in urban and highway scenarios in order to select sensor modalities, sensor type and sensor placement for automated

This research received funding from the Flemish Government under the "Onderzoeksprogramma Artificiële Intelligentie (AI) Vlaanderen" program.

driving. To the best of our knowledge, a CRLB expression taking the movement of the radar into account is not available from the literature. Therefore, we derive in this paper the CRLB for position and velocity estimation of a moving target based on a sequence of noisy range, azimuth, and Doppler measurements taken from a moving ego-vehicle equipped with one or multiple radars. Whereas the target is assumed to move according to a deterministic dynamic model with unknown but constant parameters, the ego-vehicle can follow an arbitrary but known trajectory. We follow a practical approach where at each instant the target's state is estimated with respect to the current coordinate system (CS) of the ego-vehicle. The measurement noise is zero-mean Gaussian, but can be temporally correlated. Not only does the resulting CRLB serve as a benchmark to evaluate the performance of any unbiased estimator, it also allows to quantify the impact of frame rate and other radar configuration parameters in realistic scenarios, where the car's motion considerably affects the accuracy of the tracker. This includes the application of multiple radar sensors, as well as their position and orientation with respect to the ego-vehicle. These important practical insights are also applicable in the context of Bayesian tracking.

In addition, we assess the performance of classical estimators such as the least-squares estimator (LSE) and generalized least-squares estimator (GLSE). We show that the GLSE combines low complexity and excellent performance when only few measurements are available. In this case, the GLSE can also be used to improve the initialization of recursive Bayesian filters, which are known to suffer from various imperfections. For instance, the KF is known to be optimal only for a linear system with temporally white Gaussian noise with known covariance matrices [18]. PFs, which approximate the posterior density of the state by a set of random samples or particles, also require accurate knowledge of the covariance matrices of the process and measurement noise and a proper state initialization based on the a priori distribution of the state. In practice, these conditions are rarely met, resulting in convergence issues and degraded overall performance.

Finally, based on the derived CRLB, we propose a novel active sensing (AS) application where the radar configuration is optimized on the fly to improve either tracking accuracy or computational efficiency. The presented approach is also applicable in the context of IMM filters.

Although radar is able to provide the required measurements, the analysis is not restricted to radar only, since, e.g., accurate azimuth estimation could be obtained from vision-based pedestrian detection in a hybrid radar-camera tracking system.

II. CRLB

A. Radar Measurements

We consider a scenario where an ego-vehicle equipped with M radar sensors is following an arbitrary but known trajectory and a target which is assumed to move according to a deterministic dynamic model defined by a parameter vector $\boldsymbol{\phi} = [\phi_0, \ldots, \phi_{N-1}]^{\mathrm{T}}$ consisting of N unknown but constant

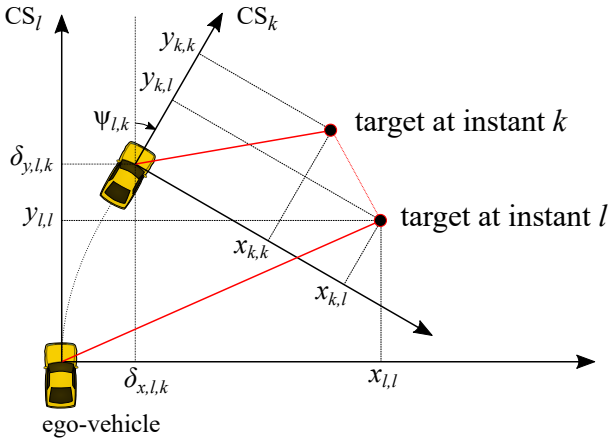

Fig. 1: A moving target as seen from a moving ego-vehicle.

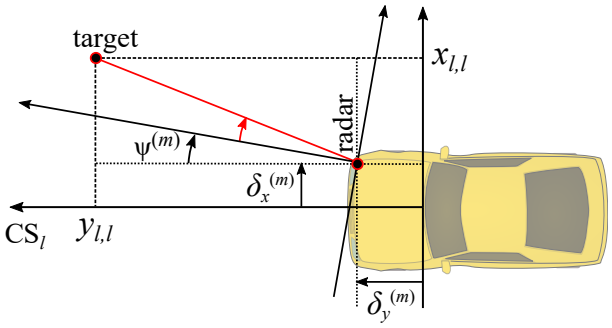

Fig. 2: Fixed position and orientation of m-th radar sensor with respect to ego-vehicle.

parameters ϕ_n. Dynamic models often used in tracking applications are the constant velocity (CV), constant acceleration (CA), and constant turn (CT) models [19]. Note that the parameters of the dynamic model depend on the choice of the CS. We follow a practical approach where the ego-vehicle is assumed to estimate $\boldsymbol{\phi}$ with respect to its current CS, which has its origin located at the ego-vehicle's current position and its y-axis directed along the ego-vehicle's current velocity vector, as shown in Fig. 1. Since the ego-vehicle is moving, this approach implies that the parameters of $\boldsymbol{\phi}$ depend on the time instant k, such that we use $\boldsymbol{\phi}_k = [\phi_{k,0}, \ldots, \phi_{k,N-1}]^{\mathrm{T}}$ to denote the parameter vector with respect to CS$_k$, the ego-vehicle's CS at time instant k. Given the dynamic model $\boldsymbol{\phi}_k$ and a frame rate $1/T$, we can easily derive the target's position and absolute velocity at each time instant l with respect to CS$_k$, which we denote by $\mathbf{p}_{k,l}(\boldsymbol{\phi}_k) = [x_{k,l}(\boldsymbol{\phi}_k), y_{k,l}(\boldsymbol{\phi}_k)]^{\mathrm{T}}$ and $\mathbf{v}_{k,l}(\boldsymbol{\phi}_k) = [\dot{x}_{k,l}(\boldsymbol{\phi}_k), \dot{y}_{k,l}(\boldsymbol{\phi}_k)]^{\mathrm{T}}$, respectively. In the remainder of the section, we will omit the dependency on $\boldsymbol{\phi}_k$ to shorten the notation. As illustrated in Fig. 2, we assume that the m-th radar has a fixed position $\boldsymbol{\delta}^{(m)} = [\delta_x^{(m)}, \delta_y^{(m)}]^{\mathrm{T}}$ and orientation $\psi^{(m)}$ with respect to the ego-vehicle's CS, with $m \in \{0, \ldots, M-1\}$. This way, the target's range, azimuth, and Doppler velocity at time instant l at the m-th radar sensor

are given by:

$$\begin{cases} \mu_{r,l}^{(m)} = \sqrt{\left(x_{l,l} - \delta_x^{(m)}\right)^2 + \left(y_{l,l} - \delta_y^{(m)}\right)^2}, \\ \mu_{\theta,l}^{(m)} = \arctan\left(\frac{x_{l,l}-\delta_x^{(m)}}{y_{l,l}-\delta_y^{(m)}}\right) - \psi^{(m)}, \\ \mu_{d,l}^{(m)} = \frac{1}{\mu_{r,l}^{(m)}}\left(\mathbf{p}_{l,l} - \boldsymbol{\delta}^{(m)}\right) \cdot (\mathbf{v}_{l,l} - \mathbf{s}_l), \end{cases} \tag{1}$$

where $\cdot$ denotes the dot product, $\mathbf{s}_l = [0, s_l]^{\mathrm{T}}$ is the ego-vehicle's velocity vector at time instant l with respect to CS_l, and $\mathbf{p}_{l,l} = [x_{l,l}, y_{l,l}]^{\mathrm{T}}$ and $\mathbf{v}_{l,l} = [\dot{x}_{l,l}, \dot{y}_{l,l}]^{\mathrm{T}}$ denote the target's position and absolute velocity at time instant l with respect to CS_l. The latter parameters are readily obtained from $\mathbf{p}_{k,l}$ and $\mathbf{v}_{k,l}$ as:

$$\begin{cases} \mathbf{p}_{l,l} = \mathbf{T}_{l,k} + \mathbf{R}_{l,k}\mathbf{p}_{k,l}, \\ \mathbf{v}_{l,l} = \mathbf{R}_{l,k}\mathbf{v}_{k,l}, \end{cases} \tag{2}$$

where the rotation matrix $\mathbf{R}_{l,k}$ and the translation matrix $\mathbf{T}_{l,k}$ are defined as:

$$\mathbf{R}_{l,k} = \begin{bmatrix} \cos(\psi_{l,k}) & \sin(\psi_{l,k}) \\ -\sin(\psi_{l,k}) & \cos(\psi_{l,k}) \end{bmatrix}, \tag{3}$$

and

$$\mathbf{T}_{l,k} = \begin{bmatrix} \delta_{x,l,k} \\ \delta_{y,l,k} \end{bmatrix}, \tag{4}$$

with $\psi_{l,k}$ and $[\delta_{x,l,k}, \delta_{y,l,k}]$ being the rotation and translation of CS_k with respect to CS_l. Since the trajectory of the ego-vehicle is assumed to be known, the matrices $\mathbf{T}_{l,k}$ and $\mathbf{R}_{l,k}$ which define the transformations between the different coordinate systems can be easily obtained. Given that $\mathbf{p}_{k,l}$ and $\mathbf{v}_{k,l}$ are a function of the dynamic model $\boldsymbol{\phi}_k$, it follows from (1) and (2) that the actual range, azimuth, and Doppler velocity at time instant l can be written as a function of the target's dynamic model $\boldsymbol{\phi}_k$.

For the sake of clarity, we introduce the vector $\boldsymbol{\mu}_l^{(m)} = [\mu_{r,l}^{(m)}, \mu_{\theta,l}^{(m)}, \mu_{d,l}^{(m)}]^{\mathrm{T}}$ which stacks the range, azimuth, and Doppler velocity from (1). By concatenating the vectors corresponding to the different radar sensors, we have $\boldsymbol{\mu}_l = [(\boldsymbol{\mu}_l^{(0)})^{\mathrm{T}}, \ldots, (\boldsymbol{\mu}_l^{(M-1)})^{\mathrm{T}}]^{\mathrm{T}}$. Assuming that at time instant k the parameter vector is estimated from the current and K previous radar measurements, we introduce the vector

$$\boldsymbol{\mu} := \boldsymbol{\mu}_{\{k-K:k\}} = [\boldsymbol{\mu}_{k-K}^{\mathrm{T}}, \ldots, \boldsymbol{\mu}_k^{\mathrm{T}}]^{\mathrm{T}}, \tag{5}$$

the length of which is $3M(K+1)$. It is important to recall that all elements of $\boldsymbol{\mu}$ depend on the parameter vector $\boldsymbol{\phi}_k$.

B. Noise Covariance Matrix

In practice, radar measurements are affected by a large variety of noise sources. Not only does FMCW radar suffer from quantization noise due to finite FFT resolution, the accuracy of radar measurements is also degraded by the low radar cross section (RCS) of VRUs, the presence of clutter, and multipath effects. Moreover, VRUs are not point targets, so at different time instances, the main reflection might come from different parts of the target, which also adversely affects tracking accuracy. In order to keep the problem analytically tractable, we consider additive zero-mean Gaussian measurement noise, such that the measurement vector $\mathbf{z}$ gathering all radar measurements from instant $k-K$ until the current instant k is given by:

$$\mathbf{z} = \boldsymbol{\mu} + \mathbf{w}, \tag{6}$$

where $\boldsymbol{\mu}$ is given by (5). The $3M(K+1) \times 3M(K+1)$ noise covariance matrix $\boldsymbol{\Sigma} = E[\mathbf{w}\mathbf{w}^{\mathrm{T}}]$ enables correlation between range, azimuth, and Doppler measurements, between radar sensors, and in time. Note that, in general, $\boldsymbol{\Sigma}$ is a function of $\boldsymbol{\phi}_k$. For instance, the measurement noise can have a larger variance for large range or azimuth. Since $\boldsymbol{\phi}_k$ is to be estimated, this implies that the tracker does not know $\boldsymbol{\Sigma}$, although it can approximate the unknown range or azimuth by range or azimuth measurements. However, regardless of dependency on $\boldsymbol{\phi}_k$, finding a good estimate for $\boldsymbol{\Sigma}$ is a challenging task given the constantly changing environment of a moving vehicle. Therefore, a detailed analysis of $\boldsymbol{\Sigma}$ is outside the scope of this paper.

C. Fisher Information Matrix

The CRLB for the unknown parameters of the dynamic model can be obtained from the Fisher Information Matrix (FIM). All radar measurements are gathered in the vector $\mathbf{z}$ and distributed according to $\mathbf{z} \sim N(\boldsymbol{\mu}, \boldsymbol{\Sigma})$. In the general case that both $\boldsymbol{\mu}$ and $\boldsymbol{\Sigma}$ are a function of the unknown variables in $\boldsymbol{\phi}_k$, we can use the Slepian-Bangs formula to obtain the (i,j)-th element of the FIM [20], [21]:

$$[\mathbf{I}(\boldsymbol{\phi}_k)]_{i,j} = \frac{\partial \boldsymbol{\mu}^{\mathrm{T}}}{\partial \phi_{k,i}} \boldsymbol{\Sigma}^{-1} \frac{\partial \boldsymbol{\mu}}{\partial \phi_{k,j}} + \frac{1}{2}\mathrm{tr}\left(\boldsymbol{\Sigma}^{-1}\frac{\partial \boldsymbol{\Sigma}}{\partial \phi_{k,i}}\boldsymbol{\Sigma}^{-1}\frac{\partial \boldsymbol{\Sigma}}{\partial \phi_{k,j}}\right). \tag{7}$$

For a covariance matrix $\boldsymbol{\Sigma}$ that is independent of $\boldsymbol{\phi}_k$, the second term in (7) becomes zero. Under the latter assumption, we can further simplify (7) by assuming that certain measurements are conditionally independent. For instance, if the noise on different radar sensors is uncorrelated, (7) reduces to the sum of the FIMs corresponding to these radar sensors. In order to calculate the CRLB for unbiased estimators not using one or multiple observations, it is sufficient to remove these observations from $\boldsymbol{\mu}$ and to remove the corresponding rows and columns from $\boldsymbol{\Sigma}$.

For each of the unknown variables in $\boldsymbol{\phi}_k$, the CRLB for any unbiased estimator can be obtained from the FIM as follows:

$$E\left[\left|\hat{\phi}_{k,i} - \phi_{k,i}\right|^2\right] \geqslant \left[\mathbf{I}(\boldsymbol{\phi}_k)^{-1}\right]_{i,i}, \tag{8}$$

where the elements of $\mathbf{I}(\boldsymbol{\phi}_k)$ are given by (7).

III. Practical Estimators

It follows from (6) that the parameter vector $\boldsymbol{\phi}_k$ can be found by minimizing the squared residuals between the radar measurements in $\mathbf{z}$ and the actual values for range, azimuth and relative radial velocity in $\boldsymbol{\mu}(\boldsymbol{\phi}_k)$:

$$\hat{\boldsymbol{\phi}}_k = \arg\min_{\tilde{\boldsymbol{\phi}}} \left\|\mathbf{z} - \boldsymbol{\mu}(\tilde{\boldsymbol{\phi}})\right\|^2, \tag{9}$$

where we again explicitly mention the dependency of the vector $\boldsymbol{\mu}$ from (5) on the target's (unknown) dynamic model $\boldsymbol{\phi}_k$. Since it follows from (1) that $\boldsymbol{\mu}(\boldsymbol{\phi}_k)$ is a non-linear function, (9) is a non-linear least-squares (LS) problem. Since a closed-form solution cannot be obtained, we linearize $\boldsymbol{\mu}(\boldsymbol{\phi}_k)$ around a certain initial estimate $\hat{\boldsymbol{\phi}}_{k,0}$:

$$\boldsymbol{\mu}\left(\boldsymbol{\phi}_k\right) = \boldsymbol{\mu}\left(\hat{\boldsymbol{\phi}}_{k,0}\right) + \mathbf{H}_0\left(\boldsymbol{\phi}_k - \hat{\boldsymbol{\phi}}_{k,0}\right), \tag{10}$$

where the Jacobian $\mathbf{H}_0$ is given by

$$\mathbf{H}_0 = \left[\frac{\partial \boldsymbol{\mu}\left(\boldsymbol{\phi}\right)}{\partial \phi_j}\right]_{\boldsymbol{\phi}=\hat{\boldsymbol{\phi}}_{k,0}} \tag{11}$$

and the initial estimate $\hat{\boldsymbol{\phi}}_{k,0}$ can be found using a naive suboptimal estimator. Using the linear approximation (10), the well-known LSE is given by:

$$\hat{\boldsymbol{\phi}}_k^{\mathrm{LS}} = \hat{\boldsymbol{\phi}}_{k,0} + \left(\mathbf{H}_0^{\mathrm{T}}\mathbf{H}_0\right)^{-1}\mathbf{H}_0^{\mathrm{T}}\left(\mathbf{z} - \boldsymbol{\mu}\left(\hat{\boldsymbol{\phi}}_{k,0}\right)\right). \tag{12}$$

Note that we can consider (12) as the first iteration of an iterative estimator:

$$\hat{\boldsymbol{\phi}}_{k,i+1}^{\mathrm{LS}} = \hat{\boldsymbol{\phi}}_{k,i}^{\mathrm{LS}} + \left(\mathbf{H}_i^{\mathrm{T}}\mathbf{H}_i\right)^{-1}\mathbf{H}_i^{\mathrm{T}}\left(\mathbf{z} - \boldsymbol{\mu}\left(\hat{\boldsymbol{\phi}}_{k,i}^{\mathrm{LS}}\right)\right), \tag{13}$$

which is equivalent to the so-called Gauss-Newton algorithm that is commonly used to solve non-linear least-squares problems. Assuming additive Gaussian measurement noise with known covariance matrix $\boldsymbol{\Sigma}$, further performance improvement can be achieved by replacing the LSE by the GLSE. However, since iterative algorithms are often not preferred due to computational complexity and we show in the numerical results section that very good results can be obtained after one iteration, we derive the GLSE from (12) as:

$$\hat{\boldsymbol{\phi}}_k^{\mathrm{GLS}} = \hat{\boldsymbol{\phi}}_{k,0} + \left(\mathbf{H}_0^{\mathrm{T}}\boldsymbol{\Sigma}^{-1}\mathbf{H}_0\right)^{-1}\mathbf{H}_0^{\mathrm{T}}\boldsymbol{\Sigma}^{-1}\left(\mathbf{z} - \boldsymbol{\mu}\left(\hat{\boldsymbol{\phi}}_{k,0}\right)\right). \tag{14}$$

If the linear model (10) was exact, the GLSE would be the minimum variance unbiased estimator (MVUE) for $\boldsymbol{\phi}_k$. For non-Gaussian measurement noise, the GLSE would still be the best linear unbiased estimator (BLUE). Note that although the GLSE is unbiased with respect to (10), it may be biased with respect to the actual non-linear model (1). In the case of a diagonal noise covariance matrix (uncorrelated noise), the GLSE reduces to the weighted least-squares estimator (WLSE).

IV. Active Sensing

In most state-of-the art ADAS, the radar configuration is fixed. However, by adopting an adaptive radar configuration, the tracker performance can be improved. Using the theoretical CRLB (8), we propose an AS approach where at each instant the optimal configuration is selected from a set of possible radar configurations. In this way, we can either minimize the CRLB for a specific parameter or a combination of CRLBs for different parameters, or minimize the computational complexity for a given CRLB threshold. Note that this approach assumes that the covariance matrix $\boldsymbol{\Sigma}$ depends on the radar configuration, e.g., a configuration with lower range resolution will result in a larger variance for the range measurement noise.

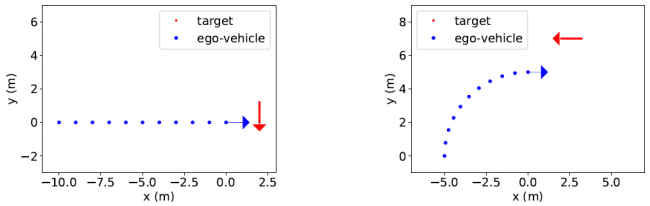

(a) Trajectory 1 (b) Trajectory 2

Fig. 3: Simulated trajectories of ego-vehicle and target. The arrow represents the velocity vector during the last radar measurement.

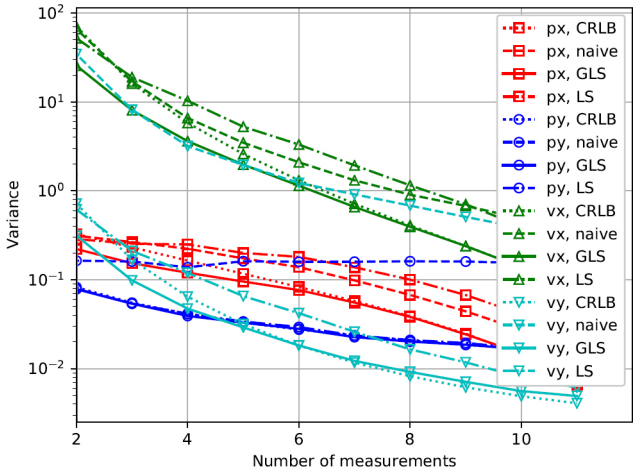

Fig. 4: CRLB for position and velocity estimation versus variance of practical estimators.

V. Numerical Results

The first example demonstrates the important scenario of a car driving at a constant velocity of 10m/s and a pedestrian crossing the street at a constant speed of 1.2m/s, as shown in Fig. 3a. Hereby, we assume that the last shown states for car and pedestrian correspond to time instant $k = 0$, at which the CRLB is calculated. In this way, the starting point of both trajectories will depend on the number of (past) measurements, whereas the endpoint (at $k = 0$) is fixed. The CRLB (8) for position and velocity estimation and the simulated variance of multiple practical estimation algorithms are displayed in Fig. 4 as a function of the number of measurements. The pedestrian's position and velocity are modeled by a CV dynamic model where, at each instant k, the parameter vector $\boldsymbol{\phi}_k = [p_{x,k}, p_{y,k}, v_{x,k}, v_{y,k}]^{\mathrm{T}}$ is estimated with respect to the ego-vehicle's current CS_k. The range, azimuth, and Doppler

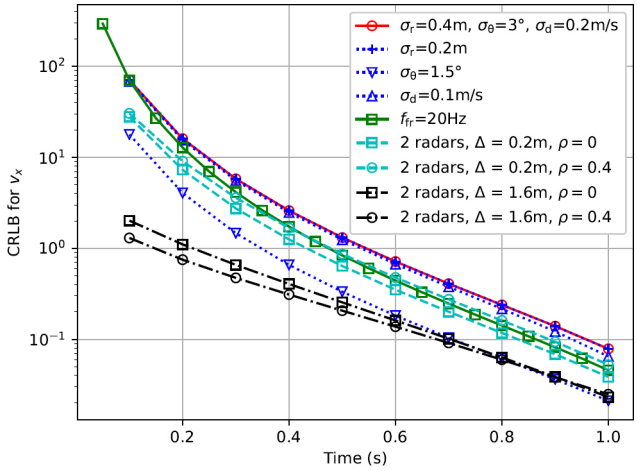

Fig. 5: CRLB for v_x for multiple radar setups and configurations.

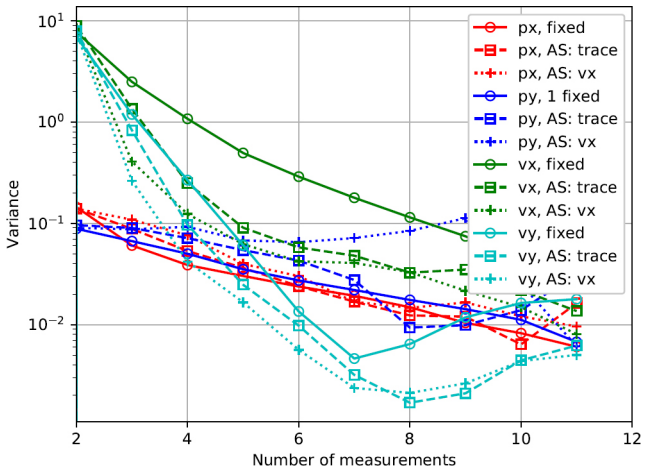

Fig. 6: Active Sensing technique using GLSE with adaptive radar configuration.

measurements are assumed to be uncorrelated and affected by AWGN with standard deviations $\sigma_r = 0.4$m, $\sigma_\theta = 0.052$ (3°), and $\sigma_d = 0.2$m/s, respectively. The radar operates at 10 fps ($T = 0.1$s). Obviously, increasing the number of measurements reduces the CRLB, although the impact of the number of measurements is much larger for velocity than for position estimation. This follows intuitively from the fact that the object's position can be obtained from a single measurement, whereas subsequent measurements are required to estimate the direction in which the object is moving, even if the radial velocity is known. Furthermore, given that Doppler measurements capture radial rather than lateral movement, it is no surprise that p_y and v_y can be more accurately estimated than p_x and v_x, thereby omitting the index k for notational convenience. In the considered scenario, the GLSE shows excellent performance after one iteration and for a small number of measurements even slightly outperforms the CRLB, which implies an estimation bias. The LSE performs remarkably worse, in most cases even worse than a naive estimator, which does not use Doppler measurements and estimates the position from the current range and azimuth measurements and the velocity from the first and last available positions. Simulations with more than one iteration for the GLSE and LSE showed very little performance improvement. In order not to overload the figure, these curves are not displayed.

In order to avoid a potential collision in the above scenario, it is essential to have an accurate estimate of v_x (perpendicular to the ego-vehicle's trajectory). However, since it follows from Fig. 4 that even the best practical estimator for v_x will show relatively low accuracy, it is important to reduce the CRLB by a proper radar setup and/or configuration. In Fig. 5, we show the CRLB for v_x for multiple radar setups and configurations. For instance, it follows from the figure that halving the standard deviation of the noise on range and Doppler measurements has a negligible impact on the CRLB. More accurate azimuth measurements, however, result in a much lower CRLB. This motivates the use of (computationally demanding) superresolution techniques such as MUSIC to estimate the azimuth or even radar-camera sensor fusion, since cameras are known to deliver very accurate azimuth information. In order to investigate the impact of a higher frame rate, we display the CRLB versus time, to allow a fair comparison. However, since the accuracy of velocity estimation largely depends on the total movement of the pedestrian, the effect of increasing the frame rate is rather small. A much more effective solution consist of mounting two radars that are separated as far as possible. For instance, whereas a separation of 0.2m ($\delta_x^{(0)} = -0.1$m, $\delta_x^{(1)} = 0.1$m) results in a minor improvement of the CRLB, two radars separated by 1.6m ($\delta_x^{(0)} = -0.8$m, $\delta_x^{(1)} = 0.8$m) achieve impressive results compared to the case of a single radar. After 0.2s, e.g., the CRLB is reduced by a factor larger than 10. Furthermore, the impact of correlation between the radars is rather small and could even be beneficial, provided that the correlation coefficient is known.

Fig. 6 displays the simulated variance of the position and velocity estimates as a function of the number of available measurements. The ego-vehicle is assumed to take a right turn with 5m-radius at a constant speed of 7.85m/s, whereas the pedestrian follows a CV model with speed 1.2m/s, as shown in Fig. 3b. We assume an AS approach where the ego-vehicle is equipped with two radars that are separated by 1.6m, and at each time step k the radar configuration for the next measurement at instant $k+1$ is selected such that either the CRLB for a particular parameter (in this case, v_x) or a combination of the CRLBs corresponding to different parameters (in this case, the trace of the inverse FIM from

(8)) is minimized. In order to calculate the CRLB, we predict the parameter vector $\hat{\boldsymbol{\phi}}_{k+1}$ based on the current estimate $\hat{\boldsymbol{\phi}}_k$. The ego-vehicle's position and velocity at instant $k+1$ are assumed to be known although in practice they need to be predicted from the trajectory up to instant k. For the fixed radar configuration scheme, we use the same standard deviations $\sigma_r = 0.4$m, $\sigma_\theta = 0.052$ (3°), and $\sigma_d = 0.2$m/s as for the previous examples. In the AS approach, however, it is assumed that range resolution can be traded for Doppler resolution, resulting in two additional configurations giving rise to $\sigma_r = 0.1$m and $\sigma_d = 0.8$m/s, and $\sigma_r = 1.6$m and $\sigma_d = 0.05$m/s, respectively. The standard deviation of the azimuth measurements remains constant. With two radars and three possible configurations for each, 9 different combinations of radar configurations can be selected. When minimizing the CRLB for v_x, it is observed from the figure that after 4 measurements, the variance on v_x is almost 10 times lower than in the case of a fixed configuration. Although the variances of the estimates of p_x and v_y are also satisfactory, the variance of the estimate of p_y becomes much worse after more than 5 measurements. To avoid this, we can minimize the sum of the CRLBs (i.e., the trace of the inverse FIM) for the four parameters of the CV model. Although the variance on v_x becomes slightly larger, the variance on p_y is much lower.

VI. Conclusion

In this paper, we derived the Cramer-Rao lower bound (CRLB) for position and velocity estimation of a moving target based on a sequence of noisy range, azimuth, and Doppler measurements taken from a moving ego-vehicle equipped with one or multiple radars. We showed how these expressions allowed to gain interesting and important practical insights regarding the impact of radar position and configuration on the accuracy of radar based VRU perception systems. Furthermore, we showed that the generalized least-squares estimator (GLSE) achieves excellent performance when few measurements are available, and introduced an active sensing (AS) application based on the CRLB where the radar configuration is optimized on the fly to improve either tracking accuracy or computational efficiency.

References

[1] S. M. Patole, M. Torlak, D. Wang, and M. Ali, "Automotive radars: A review of signal processing techniques," *IEEE Signal Processing Magazine*, vol. 34, pp. 22–35, March 2017.

[2] G. Hakobyan and B. Yang, "High-performance automotive radar: A review of signal processing algorithms and modulation schemes," *IEEE Signal Processing Magazine*, vol. 36, pp. 32–44, Sep. 2019.

[3] Z. Chen and C. Tang, "Robust pedestrian tracking using interactive multiple model particle filter and feature matching," in *3rd International Conference on Advanced Robotics and Mechatronics (ICARM)*, pp. 480–485, 2018.

[4] P. Tichavsky, C. H. Muravchik, and A. Nehorai, "Posterior Cramer-Rao bounds for discrete-time nonlinear filtering," *IEEE Transactions on Signal Processing*, vol. 46, no. 5, pp. 1386–1396, 1998.

[5] M. L. Hernandez, A. D. Marrs, N. J. Gordon, S. R. Maskell, and C. M. Reed, "Cramer-Rao bounds for non-linear filtering with measurement origin uncertainty," in *Proceedings of the Fifth International Conference on Information Fusion. FUSION 2002. (IEEE Cat.No.02EX5997)*, vol. 1, pp. 18–25 vol.1, 2002.

[6] Z. Wang and X. Shen, "Posterior Cramer-Rao bounds for discrete-time nonlinear filtering with finitely correlated noises," in *2015 34th Chinese Control Conference (CCC)*, pp. 4541–4546, 2015.

[7] L. Zuo, R. Niu, and P. K. Varshney, "Conditional posterior Cramer-Rao lower bounds for nonlinear sequential Bayesian estimation," *IEEE Transactions on Signal Processing*, vol. 59, no. 1, pp. 1–14, 2011.

[8] K. L. Bell, C. J. Baker, G. E. Smith, J. T. Johnson, and M. Rangaswamy, "Cognitive radar framework for target detection and tracking," *IEEE Journal of Selected Topics in Signal Processing*, vol. 9, no. 8, pp. 1427–1439, 2015.

[9] H. Zhang, W. Liu, J. Xie, Z. Zhang, and W. Lu, "Joint subarray selection and power allocation for cognitive target tracking in large-scale MIMO radar networks," *IEEE Systems Journal*, vol. 14, no. 2, pp. 2569–2580, 2020.

[10] M. Xie, W. Yi, T. Kirubarajan, and L. Kong, "Joint node selection and power allocation strategy for multitarget tracking in decentralized radar networks," *IEEE Transactions on Signal Processing*, vol. 66, no. 3, pp. 729–743, 2018.

[11] Z. Li, J. Xie, H. Zhang, H. Xiang, and C. Wang, "Joint beam selection and resource allocation for cognitive multiple targets tracking in MIMO radar with collocated antennas," *IET Radar, Sonar and Navigation*, vol. 14, no. 12, pp. 2000–2009, 2020.

[12] H. Godrich, A. M. Haimovich, and R. S. Blum, "Target localization accuracy gain in MIMO radar-based systems," *IEEE Transactions on Information Theory*, vol. 56, no. 6, pp. 2783–2803, 2010.

[13] A. A. Gorji, R. Tharmarasa, W. D. Blair, and T. Kirubarajan, "Multiple unresolved target localization and tracking using colocated MIMO radars," *IEEE Transactions on Aerospace and Electronic Systems*, vol. 48, no. 3, pp. 2498–2517, 2012.

[14] N. Rojhani, M. S. Greco, and F. Gini, "Target range and velocity CRLBs for colocated MIMO radar in CES disturbance," in *2022 IEEE 12th Sensor Array and Multichannel Signal Processing Workshop (SAM)*, pp. 385–389, 2022.

[15] M. Karan and R. N. Lobbia, "Cramer-Rao lower bound for single target tracking accuracy with coordinated turn maneuvers using range and bearing measurements," in *Sixth International Conference of Information Fusion, 2003. Proceedings of the*, vol. 2, pp. 911–918, July 2003.

[16] M. A. Smith, "On Doppler measurements for tracking," in *2008 International Conference on Radar*, pp. 513–518, 2008.

[17] J. Domhof, R. Happee, and P. P. Jonker, "Multi-sensor object tracking performance limits by the Cramer-rao lower bound," *2017 20th International Conference on Information Fusion (Fusion)*, pp. 1–8, 2017.

[18] Z. Chen, "Bayesian filtering: From kalman filters to particle filters, and beyond," *Statistics*, vol. 182, 01 2003.

[19] X. Rong Li and V. P. Jilkov, "Survey of maneuvering target tracking. part i. dynamic models," *IEEE Transactions on Aerospace and Electronic Systems*, vol. 39, no. 4, pp. 1333–1364, 2003.

[20] D. Slepian, "Estimation of signal parameters in the presence of noise," *Transactions of the IRE Professional Group on Information Theory*, vol. 3, no. 3, pp. 68–89, 1954.

[21] W. J. Bangs, "Array processing with generalized beamformers," 1971.